11-10-2020

A Geologically Based Indoor-Radon Potential Map of Kentucky

William C. Haneberg
University of Kentucky, bill.haneberg@uky.edu

Amanda T. Wiggins
University of Kentucky, amandathaxtonwiggins@gmail.com

Douglas C. Curl
University of Kentucky, doug@uky.edu

Stephen F. Greb
University of Kentucky, greb@uky.edu

William M. Andrews Jr.
University of Kentucky, wandrews@uky.edu

See next page for additional authors

Citation Information

Published in GeoHealth, v. 4, issue 11, e2020GH000263.

A Geologically Based Indoor-Radon Potential Map of Kentucky

Digital Object Identifier (DOI)
https://doi.org/10.1029/2020gh000263

Authors
William C. Haneberg, Amanda T. Wiggins, Douglas C. Curl, Stephen F. Greb, William M. Andrews Jr., Kathy Rademacher, Mary Kay Rayens, and Ellen J. Hahn

GeoHealth

RESEARCH ARTICLE
10.1029/2020GH000263

A Geologically Based Indoor-Radon Potential Map of Kentucky

William C. Haneberg[1], Amanda Wiggins[2], Douglas C. Curl[1], Stephen F. Greb[1], William M. Andrews Jr.[1], Kathy Rademacher[2], Mary Kay Rayens[2], and Ellen J. Hahn[2,3]

[1]Kentucky Geological Survey, University of Kentucky, Lexington, KY, USA, [2]BREATHE, College of Nursing, University of Kentucky, Lexington, KY, USA, [3]Center for Appalachian Research in Environmental Sciences, University of Kentucky, Lexington, KY, USA

Key Points:
- Bedrock geologic units in Kentucky have lithologically controlled indoor-radon potential
- Carbonate sedimentary rocks generally have higher indoor-radon potential than nonshale clastic sediments and sedimentary rocks
- We used geologic map coverage and radon test results to produce an interactive statewide indoor-radon potential map for nonspecialists

Supporting Information:
- Supporting Information S1
- Table S1

Correspondence to:
W. C. Haneberg,
bill.haneberg@uky.edu

Citation:
Haneberg, W. C., Wiggins, A., Curl, D. C., Greb, S. F., Andrews, W. M. Jr., Rademacher, K., et al. (2020). A geologically based indoor-radon potential map of Kentucky. *GeoHealth*, *4*, e2020GH000263. https://doi.org/10.1029/2020GH000263

Received 27 APR 2020
Accepted 2 NOV 2020
Accepted article online 10 NOV 2020

Author Contributions:
Conceptualization: Ellen J. Hahn
Data curation: Douglas C. Curl
Formal analysis: William C. Haneberg, Amanda Wiggins, Stephen F. Greb, Kathy Rademacher, Mary Kay Rayens
Funding acquisition: Ellen J. Hahn
Investigation: Stephen F. Greb, William M. Andrews Jr.
Methodology: William C. Haneberg, Amanda Wiggins, Douglas C. Curl, Stephen F. Greb, William M. Andrews Jr., Kathy Rademacher, Mary Kay Rayens, Ellen J. Hahn
(continued)

Abstract We combined 71,930 short-term (median duration 4 days) home radon test results with 1:24,000-scale bedrock geologic map coverage of Kentucky to produce a statewide geologically based indoor-radon potential map. The test results were positively skewed with a mean of 266 Bq/m^3, median of 122 Bq/m^3, and 75th percentile of 289 Bq/m^3. We identified 106 formations with ≥10 test results. Analysis of results from 20 predominantly monolithologic formations showed indoor-radon concentrations to be positively skewed on a formation-by-formation basis, with a proportional relationship between sample means and standard deviations. Limestone (median 170 Bq/m^3) and dolostone (median 130 Bq/m^3) tended to have higher indoor-radon concentrations than siltstones and sandstones (median 67 Bq/m^3) or unlithified surficial deposits (median 63 Bq/m^3). Individual shales had median values ranging from 67 to 189 Bq/m^3; the median value for all shale values was 85 Bq/m^3. Percentages of values falling above the U.S. Environmental Protection Agency (EPA) action level of 148 Bq/m^3 were sandstone and siltstone: 24%, unlithified clastic: 21%, dolostone: 46%, limestone: 55%, and shale: 34%. Mississippian limestones, Ordovician limestones, and Devonian black shales had the highest indoor-radon potential values in Kentucky. Indoor-radon test mean values for the selected formations were also weakly, but statistically significantly, correlated with mean aeroradiometric uranium concentrations. To produce a map useful to nonspecialists, we classified each of the 106 formations into five radon-geologic classes on the basis of their 75th percentile radon concentrations. The statewide map is freely available through an interactive internet map service.

Plain Language Summary Exposure to high levels of radon is the second leading cause of lung cancer in the United States and greatly increases the likelihood of lung cancer in people who are also exposed to tobacco smoke. Produced by the radioactive decay of naturally occurring uranium in rocks, radon gas migrates into homes where it and its radioactive decay products can be inhaled by humans. We know that different kinds of bedrock produce different amounts of radon. To illustrate the danger posed by indoor radon in Kentucky, we combined results from 71,930 radon home test kits with geologic maps showing different kinds of bedrock and produced a geologically based and highly interactive indoor-radon potential map of Kentucky. Our map is available as a web-based interactive service hosted by the Kentucky Geological Survey and requires only a desktop or mobile web browser to use. The map also includes links to supplemental information that users can access to better understand the indoor-radon danger in their counties, encourage them to have their homes tested, and, if appropriate, mitigate the problem.

1. Introduction

More than 225,000 new cases of lung cancer and almost 143,000 deaths from lung cancer were estimated to have occurred in 2019 in the United States (American Cancer Society, 2019). Radon gas—a geogenic carcinogen produced by the radioactive decay of naturally occurring uranium in rocks and sediments—is the second leading cause of lung cancer in the United States (Al-Zoughool & Krewski, 2009). Exposure to both radon and tobacco smoke increases the probability of lung cancer: The lifetime risk of radon-induced lung cancer when exposed to 148 Bq/m^3 of indoor radon is 62 per 1,000 ever smokers compared to 7 per 1,000 never smokers (Mendez et al., 2011; U.S. Environmental Protection Agency, 2009). Among never smokers, exposure to radon may be more harmful for those exposed to secondhand smoke (Lagarde et al., 2001). Recent studies have also suggested relationships between radon exposure and both breast cancer risk and

Project administration: William C. Haneberg, Ellen J. Hahn
Software: Douglas C. Curl
Supervision: William M. Andrews Jr., Ellen J. Hahn
Writing - original draft: William C. Haneberg, Douglas C. Curl, Stephen F. Greb, William M. Andrews Jr., Ellen J. Hahn
Writing – review & editing: William C. Haneberg, Amanda Wiggins, Douglas C. Curl, Stephen F. Greb, William M. Andrews Jr., Kathy Rademacher, Mary Kay Rayens, Ellen J. Hahn

malignant melanoma, or skin cancer, mortality (Vienneau, 2017; VoPham et al., 2017). Despite these statistics, few homeowners are aware of the combined environmental risk of exposure to both tobacco smoke and radon. The combination of synergistic risk and lack of homeowner awareness is a significant public health concern in Kentucky, which is (1) underlain by Paleozoic sedimentary bedrock with high radon potential in some units (Hahn et al., 2015) and (2) a national leader in smoking rates (U.S. Department of Health, & Human Services, Centers for Disease Control, & Prevention, 2018) and cancer cases (Kentucky Cancer Registry, 2017).

1.1. Purpose

This paper describes our development of a geologically based interactive map of indoor-radon potential in Kentucky as part of a public health strategy to reduce lung cancer rates by promoting radon testing and mitigation of homes with high indoor-radon levels. While there are many interesting and potentially fruitful lines of research related to lithologic, stratigraphic, and structural geologic controls on indoor-radon levels in Kentucky and elsewhere, our primary objective is to describe how we developed the map as a geologically based public health awareness tool.

Overfield et al. (2016) previously described the transdisciplinary collaboration behind ongoing radon awareness programs in Kentucky. Development of the geologically based map of indoor-radon potential in Kentucky grew out of that collaboration. Our map is novel because it (1) is based upon a large number of indoor-radon test results ($N = 71{,}930$, equating to an average of one radon test result per 0.69 km^2 across the entire state), (2) takes advantage of Kentucky's unique statewide 1:24,000-scale digital geologic mapping rather than using administrative units such as counties or census tracts as a framework for radon-potential mapping, and (3) uses a multimedia approach to disseminate radon-potential information using a highly interactive internet map service that is freely accessible to the public.

An earlier analysis of 60,763 of these indoor-radon tests resulted in county-level map infographics disseminated via the University of Kentucky's BREATHE initiative website (http://www.breathe.uky.edu). Separately published research has shown that disseminating the county-level maps based on the approach described in this paper may, even at currently low levels of mitigation, lead to an estimated savings of one life lost from lung cancer and $3.4 million to $8.5 million per year in net present-value health care costs in Kentucky (Chiavacci et al., 2020). The interactive map that we describe in this paper is part of a wider ongoing effort, including a new requirement for Kentucky real estate sellers to disclose radon test results, to increase those annual savings by encouraging residents to test and, if appropriate, mitigate their homes.

1.2. Previous Work

Radon-potential maps used for public health work in the United States, including Kentucky, have historically been based on regional bedrock geology, soil, airborne radiometry, and housing stock data combined with limited numbers of indoor-radon test results to produce a single radon hazard estimate for each county (Schumann, 1993; U.S. Environmental Protection Agency, 1993). In Kentucky, the average county area is on the order of 1,000 km^2, so assigning a single value to an entire county provides only a coarse indication of indoor-radon potential (Figure 1).

Other studies have examined variations in indoor-radon concentrations both within and between different bedrock or sediment types and at different map scales in Norway (Smethurst et al., 2008; Sundal et al., 2004), Great Britain (Miles & Appleton, 2005), Oregon (Burns et al., 1998; Franczyk et al., 2018), Russia (Zhukovsky et al., 2012), Romania (Florică et al., 2020), and part of northern Kentucky (Hahn et al., 2015). The work described by Hahn et al. (2015) is particularly relevant to this paper because it was a pilot project that provided the geological and statistical basis for the current geologically based radon-potential map of Kentucky. Their preliminary work showed Quaternary surficial deposits and Paleozoic sedimentary bedrock units mapped at a scale of 1:24,000 could be assigned to categories with significantly different indoor-radon distributions.

1.3. Geologic Setting

The near-surface geology of Kentucky comprises primarily flat-lying limestone, shale, sandstone, siltstone, dolostone, and coal ranging in age from Ordovician to Pennsylvanian (McDowell, 1986; McFarlan, 1943). Each of these rock types contains different combinations of constituent minerals, some of which contain

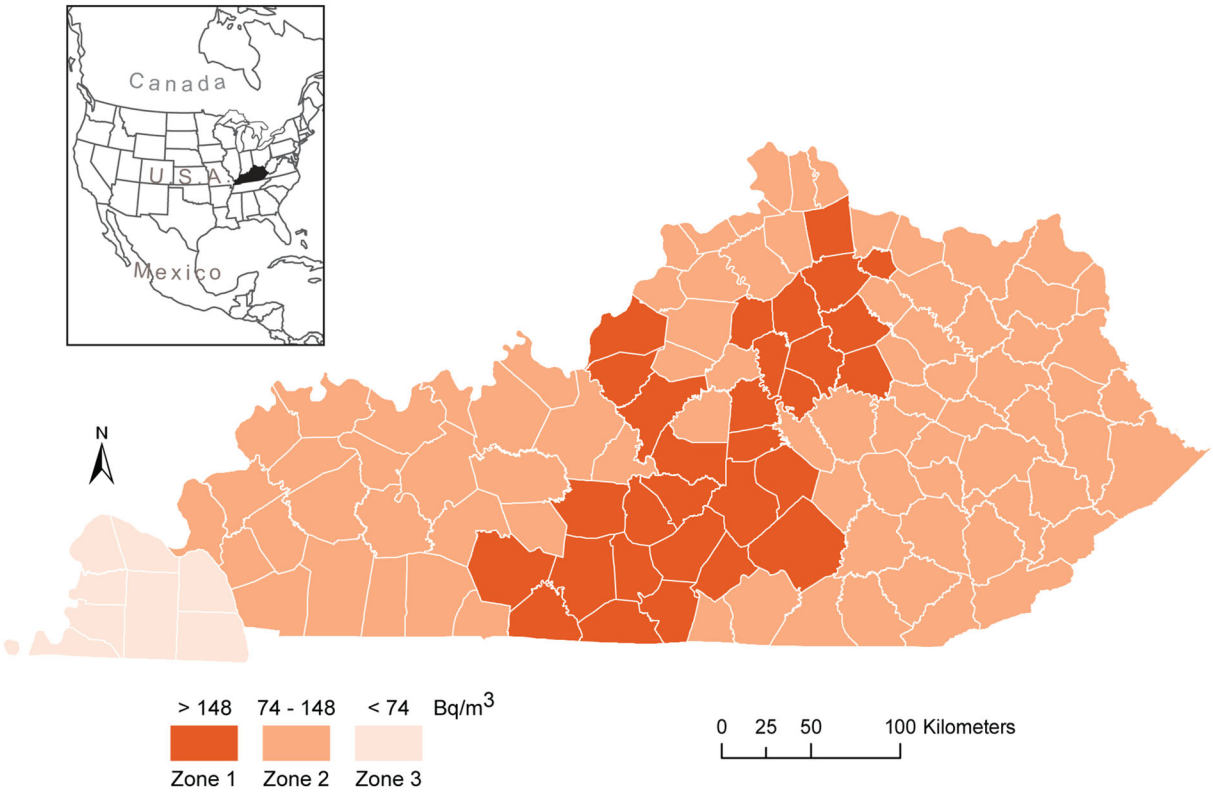

Figure 1. Radon potential of Kentucky by county, produced using 1993 U.S. Geological Survey and U.S. Environmental Protection Agency data.

trace amounts of uranium, the parent element in the radioactive decay series that produces radon. Some of the shales have large proportions of clay, which can impede the migration of fluids and gases (including radon), whereas some limestones are characterized by extensive cave and fracture systems that facilitate fluid and gas migration.

As shown in Figure 2, a simplified geologic map produced from a digital statewide 1:24,000-scale coverage (Anderson et al., 2004) and based on the joint Kentucky Geological Survey-U.S. Geological Survey geologic mapping project (McDowell, 1986), the oldest rocks exposed in Kentucky were deposited during the Late Ordovician Period. Some of these Upper Ordovician limestones locally contain apatite and other phosphate minerals (Cressman, 1973; Karathanasis, 1991; McFarlan, 1943) that can incorporate uranium into their crystal structures. Upper Ordovician rocks are generally mixed sequences of limestone and shale. Areas of thick limestone are in some places characterized by karst features such as caves, springs, and sinkholes (Currens, 2002; Paylor & Currens, 2002; White et al., 1970). Overlying Silurian rocks are dominated by dolostone and clay-rich shale (McDowell, 1986; McFarlan, 1943). Devonian rocks in Kentucky are dominated by black shale with high clay and organic content, and trace amounts of uranium, as well as phosphate minerals (Leventhal, 1981; Leventhal & Hosterman, 1982; Perkins & Mason, 2015; Swanson, 1961). The Devonian rocks are overlain by Lower Mississippian shales and siltstones, some of which are clay rich, and some of which contain phosphate nodules and glauconite (Kepferle, 1971; Udgata, 2011; Weir et al., 1966). Middle Mississippian limestones in Kentucky are commonly characterized by extensive karst features (Currens, 2002; Dicken, 1935; Palmer, 1989; Paylor & Currens, 2002). Pennsylvanian rocks in Kentucky are predominantly shale, sandstone, coal, and thin claystones. Coals and black shales can contain trace amounts of uranium (Coveney & Glascock, 1989; Eble & Hower, 1997; Harvey, 1984). Permian sedimentary and igneous rocks, as well as Upper Cretaceous gravels, are exposed over limited parts of western Kentucky. Lower Cenozoic and Quaternary mud and sand deposited in valleys, along with windblown loess deposited on uplands, are exposed in parts of Kentucky (McDowell, 1986; McFarlan, 1943), and are shown on Figure 2 in areas where they are thick enough to obscure bedrock. The simplified geologic map does not show faults, which may influence radon gas migration through the subsurface (Dai et al., 2019), but was not considered in the development of our statewide radon potential map.

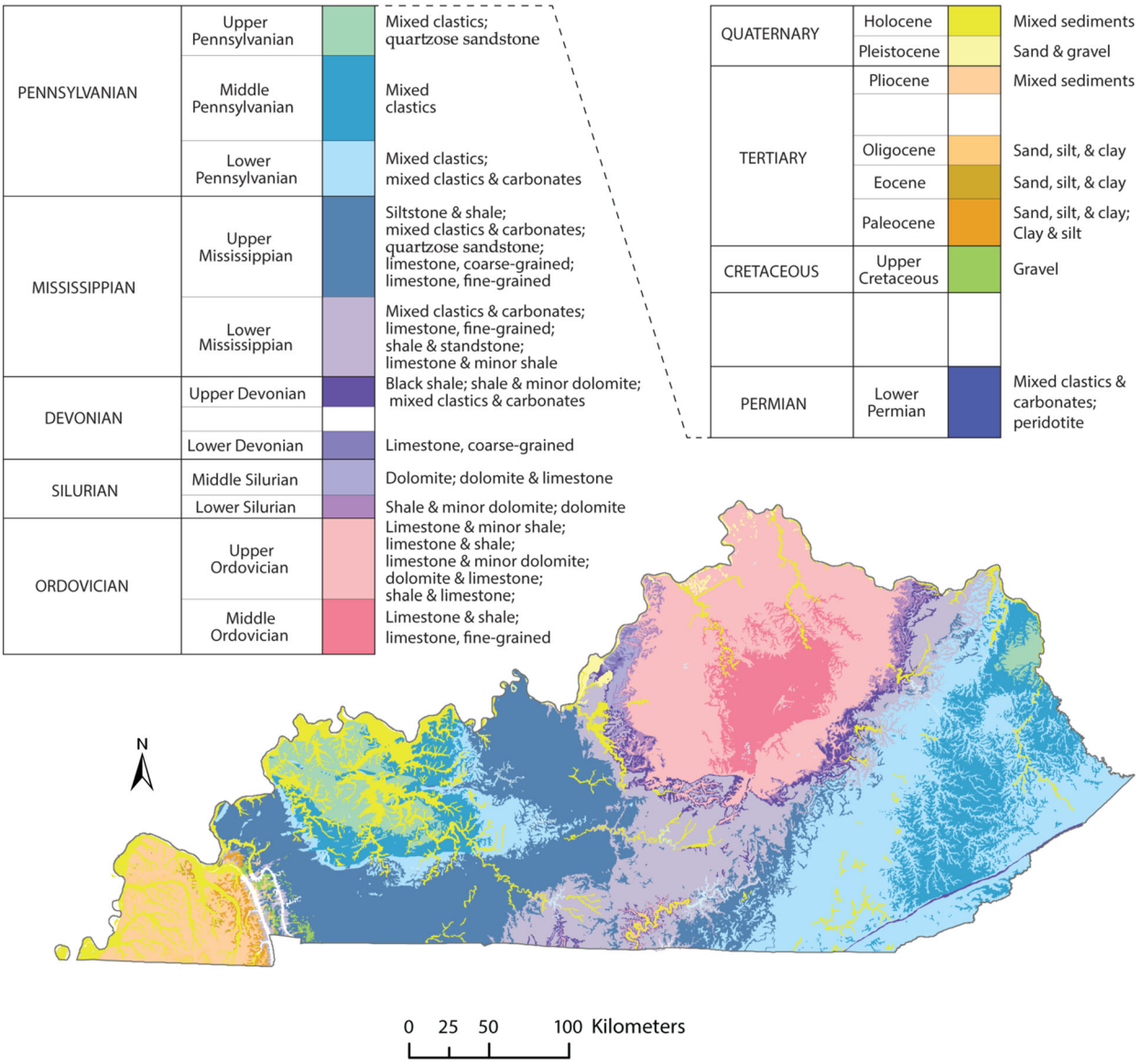

Figure 2. Simplified geology of Kentucky showing the distribution of field-mappable rock units classified according to stratigraphic position.

The outcrop patterns shown on the simplified geologic map in Figure 2 are broadly similar to those of the aeroradiometric uranium concentrations over Kentucky (Duval et al., 1993; Phillips et al., 1993) shown in Figure 3. The highest concentrations in the state, in many places >3 ppm (orange in Figure 3), occur within an arcuate belt in the center of the state that corresponds to outcrops of Devonian black shale (Figure 2). Pennsylvanian clastic rocks in the eastern portion of Kentucky generally have aeroradiometric uranium concentrations <2 ppm (green in Figure 3). Areas corresponding to Ordovician limestones, Mississippian limestones, and Quaternary alluvium tend to have large areas of aeroradiometric uranium concentrations in the range of 2 to 3 ppm.

2. Methods

We combined a vector map of radon test kit locations with the statewide 1:24,000-scale digital geologic map coverage using GIS software, assigning each home test kit location to a corresponding geologic formation using a spatial join function. We did not consider additional geologic (e.g., soil type, depth to bedrock, proximity to mapped faults, or proximity to sinkholes) or nongeologic (e.g., age of home, foundation or construction type, heating or air conditioning use, season of testing, or location of the test canister within each home)

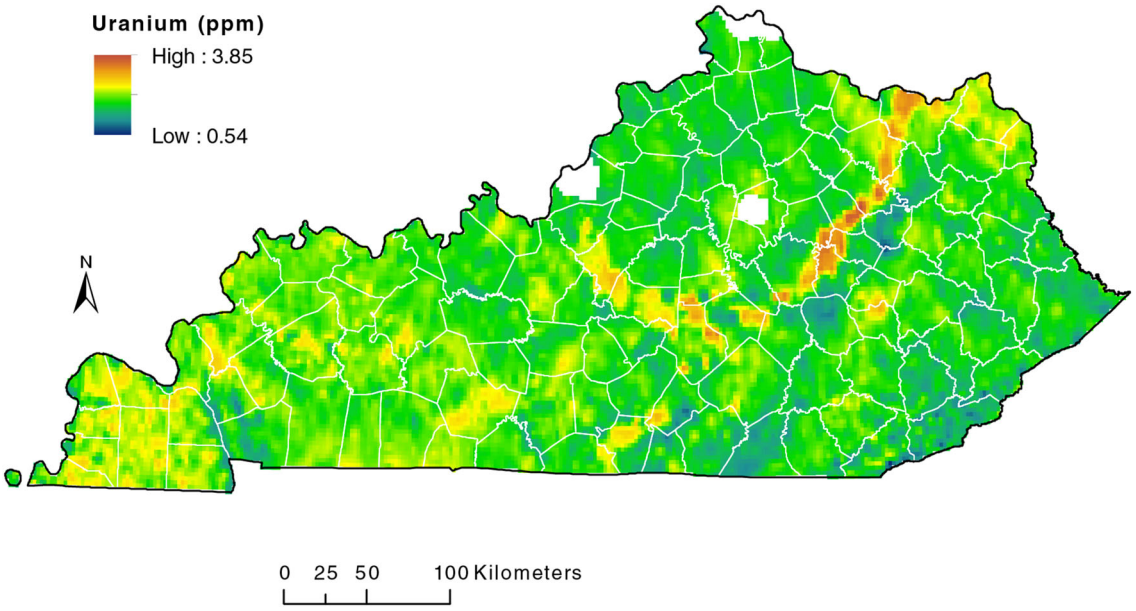

Figure 3. Aeroradiometric uranium concentration map of Kentucky. White areas within the map indicate urban areas over which data were not available. Data source: Phillips et al. (1993).

controls on indoor-radon concentrations during development of our map, although we acknowledge they may affect radon concentration and exposure levels (Otton, 1992; Tanner, 1986; U.S. Environmental Protection Agency, 1986, 2012). Those factors are all valid topics for future research and refinement of our understanding of geologic and nongeologic controls on indoor-radon levels.

After the initial mapping, formations with fewer than 10 radon test kit results were merged with similar overlying or underlying formations, based on our qualitative assessment of lithology, stratigraphy, and geographic proximity, in order to create units with enough data points to be useful for unit comparisons. The resulting merged layer contains 106 map units. We also plotted radon test results from homes built on 20 selected monolithologic units in order to evaluate the relationship between bedrock lithology, aeroradiometric uranium concentrations, and indoor-radon levels.

3. Radon Test Kit Data and Digital Geologic Map Coverage

3.1. Radon Test Kit Data

Our statewide indoor-radon potential map is based on 71,930 short-term test kit results provided by two companies that received and analyzed radon home test kits in Kentucky between 1986 and 2017. Chiavacci et al. (2020) used an earlier data set comprising 60,763 results in their economic analysis of the impact of the county-level maps on radon testing, mitigation, and health care cost savings in Kentucky from avoiding lung cancer. There are only minor differences between maps produced using the earlier data set and the one presented in this paper.

Short-term charcoal canister radon home test kits have the benefits of being quick (a minimum of 2 days is recommended), inexpensive, easily available from public health agencies or home improvement stores, minimally intrusive, and easily used by homeowners without formal training. Their most significant drawback is that single short-term tests do not provide information about long-term seasonal indoor-radon variations and may therefore not be accurate predictors of long-term radon levels (e.g., Barros et al., 2014, 2016; Groves-Kirkby et al., 2006; Stanley et al., 2019). In a detailed analysis of home radon test results from the Canadian prairie provinces, Stanley et al. (2019) showed that results of short-term tests performed during the winter months correlated to long-term 90-day test results better than those performed during the summer months.

The companies provided radon test kit identification numbers and street addresses in a separate file from the radon test results. We used an honest broker to convert street addresses to latitudes and longitudes in order

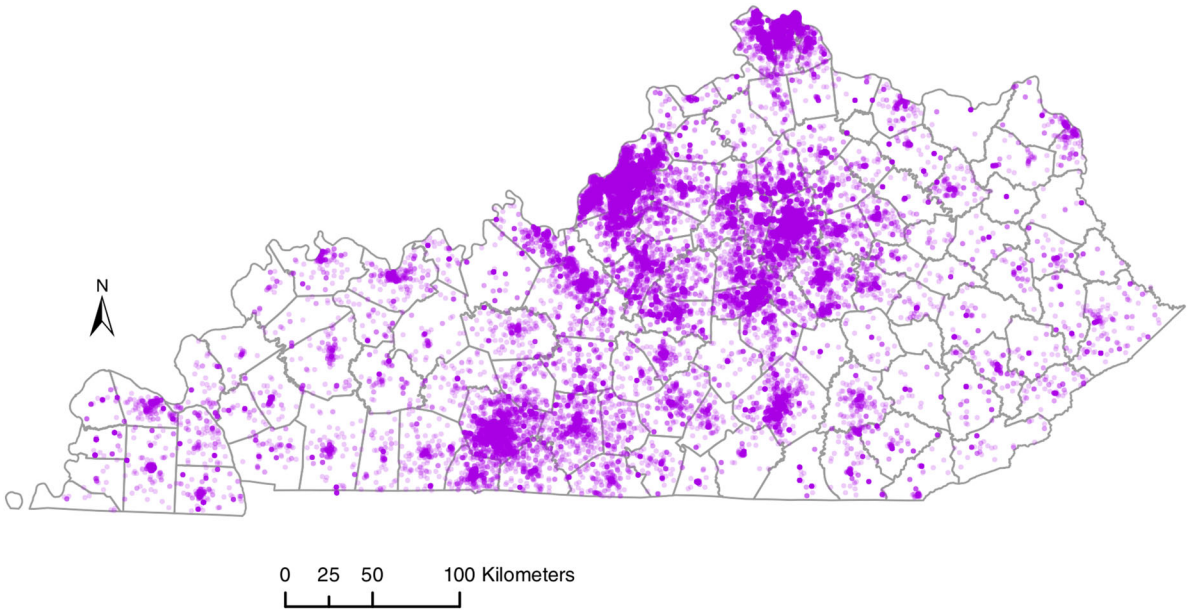

Figure 4. Locations of the 71,930 home radon test kits used as the basis for the Kentucky statewide indoor-radon potential map.

to maintain the confidentiality of residents in the tested homes. The broker reported high match rates, with 82.4% street address and 16.0% postal code match rates. Only 1.5% of the addresses yielded no match. We then combined the latitude/longitude file with the radon test results and deleted duplicate records.

The process of converting street addresses to geographic coordinates, known as geocoding, is well developed but not perfect. There are several situations in which inaccurate geographic coordinates might be assigned to a test location. First, it is possible that some test kits could have been returned with addresses different than the actual location of the home tested (e.g., a post office box). Second, especially in rural areas, the physical location of the house may be some distance from the location assigned to the street address. Third, again especially in rural areas, street addresses may be assigned to the geographic center of a postal code zone or other administrative unit if the street address is not in the geocoding database being used. For the work described in this paper, none of those complications would create a problem unless the discrepancy were large enough to place the addresses of a statistically large number of homes into a completely different geologic formation (and which we cannot evaluate without knowing the street addresses). This is a topic of ongoing research in our group.

Among the 71,930 results for which addresses were matched, there were 41,869 distinct locations with 31,051 of them having one radon measurement, 6,700 having two radon measurements, and 1,940 having three radon measurements assigned to them. A total of 50,271 test results was associated with coordinates for which three or fewer tests were reported (which could represent retesting by residents). The remainder likely represent assignments to postal code centroids. Data provided by homeowners to the testing companies show that 28,155 of test locations were in basements, 20,477 were on first floors, 857 were on second floors, and 22,441 were listed as unknown, unreported, or other. The data set contains 50,090 instances of "unknown" or "not provided" as the foundation type. The median duration of 60,583 tests for which starting and ending dates were provided by homeowners was 4 days, with 95% of the test durations of 8 days or less. The largest numbers of tests occurred in February, March, and November. The smallest numbers occurred in July and August. Of the tests for which dates could be reliably determined from the data provided by homeowners to the testing companies, a total of 37,614 (62%) was performed during the six cold weather months of October through March.

Site-specific variability aside, which we acknowledge but do not incorporate into the current radon potential map, our large data set allows for a statewide characterization of radon variability that can be compared broadly against bedrock type and age. Although all mapped geologic units in Kentucky are not represented in the data set, those that underlie large population concentrations are well represented. Figure 4 shows the

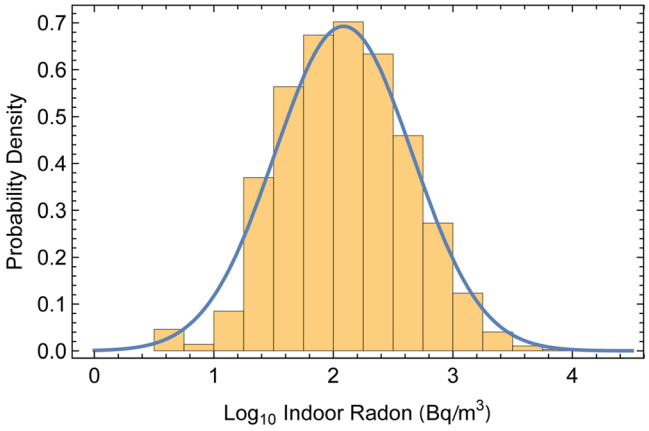

Figure 5. Histogram and normal distribution defined using the sample mean and standard deviation of 71,930 log-transformed home radon test results used for the Kentucky statewide indoor-radon potential map.

spatial distribution of test kit results and that all 120 counties in Kentucky are represented. The highest concentrations of test results are in urban and suburban centers and the lowest concentrations in sparsely populated rural counties.

3.2. Digital Statewide Geologic Coverage

A geologic map is a graphic representation of the rock units and related features (such as faults, folds, or other geologic structures) exposed at or near Earth's surface. Each polygon on a geologic map represents a different age or type of rock, and each polygon boundary line represents a transition between different rock units generically referred to as formations. From 1960 to 1978, the U.S. Geological Survey and Kentucky Geological Survey collaborated on the production of 707 geologic quadrangle maps, each covering 7.5 min of latitude and longitude, at a scale of 1:24,000, that provided complete field-based bedrock geologic map coverage of Kentucky (Cressman & Noger, 1981). From 1996 to 2004, the Kentucky Geological Survey digitized the entire set of maps and

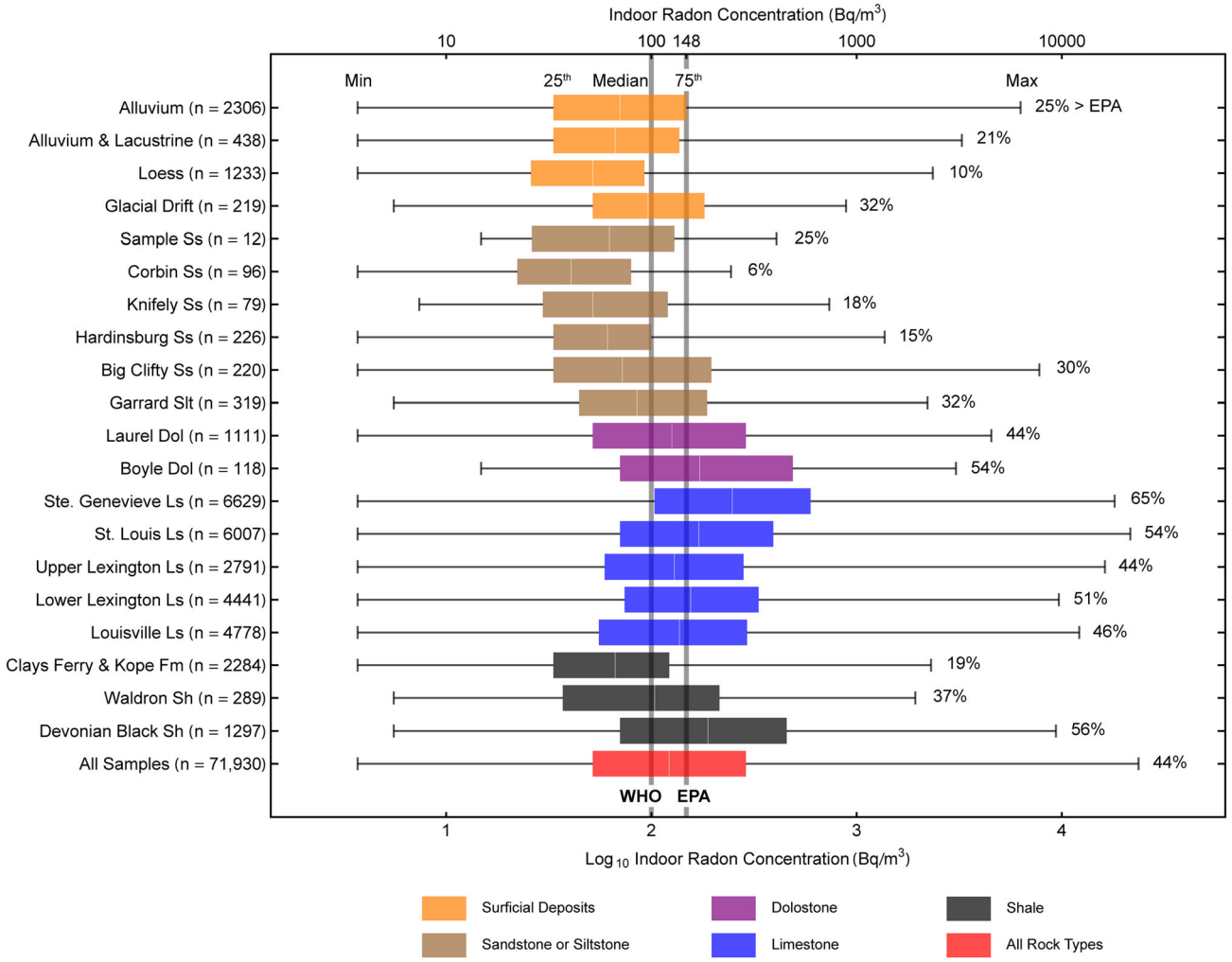

Figure 6. Distribution of indoor-radon concentrations from homes built on 20 typical bedrock and surficial deposits in Kentucky. The all-sample distribution of 71,930 points is shown at the bottom of the plot for comparison. Lithologic abbreviations used in the formation names are Ss: sandstone, Slt: siltstone, Dol: dolostone, Ls: limestone, Sh: shale. WHO: World Health Organization action level. EPA: U.S. Environmental Protection Agency action level.

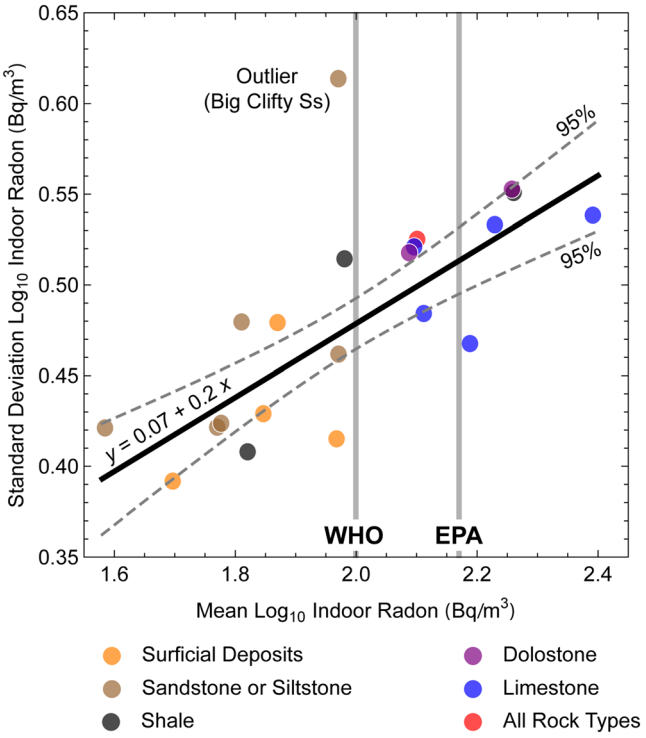

Figure 7. Mean versus standard deviation of indoor-radon concentrations in homes built on 20 typical types of bedrock and surficial deposits in Kentucky, with the all-sample distribution (red) shown for comparison. Dashed lines show the 95% mean confidence bands for the solid black best fit line. WHO: World Health Organization action level. EPA: U.S. Environmental Protection Agency action level.

produced a GIS-compatible vector data set of geologic map coverage for the state (Anderson et al., 2004). The statewide digital geologic map coverage is available to anyone with a web browser through the interactive Kentucky Geologic Map Information Service (http://kgs.uky.edu). Advanced users can download a variety of component GIS files for more sophisticated analysis.

4. Results

4.1. Sample Statistics

The radon home test kit results ($N = 71{,}930$) had a mean of 266 Bq/m^3, a median of 122 Bq/m^3, and a 75th percentile value of 289 Bq/m^3. The current World Health Organization (WHO) and U.S. Environmental Protection Agency (EPA) action levels for indoor radon are, respectively, 100 and 148 Bq/m^3. Preliminary analysis showed the radon value distribution to be positively skewed, so we used a $\log_{10}$ transform to create a symmetric normal-like data distribution to simplify subsequent data visualization and assessment (Figure 5).

Building upon the results of Hahn et al. (2015), who showed that different formations depicted on 1:24,000-scale geologic maps covering part of northern Kentucky were characterized by different distributions of indoor-radon concentrations, we selected 20 of the 106 map units for further examination. The 20 units were chosen to represent a range of bedrock and surficial deposits common in Kentucky, with an emphasis on formations whose names include specific reference to a dominant rock type (e.g., Lexington Limestone or Corbin Sandstone) or which we knew from experience to consist primarily of a single rock type (e.g., Kope Formation, which is primarily an illitic shale with minor limestone beds). This is important because formations shown on geologic maps are based on sets of characteristics—including distinctive combinations of rock types—that are observable and mappable in the field at a particular map scale. Thus, some formations may comprise two or more rock types, which might complicate the evaluation of relationships between rock type and indoor-radon potential. There may also be differences among formations comprising the same general rock types because of sedimentologic, stratigraphic, and geochemical details.

Figure 6 summarizes the distributions of the 20 selected map units and the all-sample distribution. For each of the units, the ends of each whisker denote the minimum and maximum measured concentrations, the ends of the boxes denote the 25th and 75th percentile concentrations, and the white midline within each box denotes the median (50th percentile) concentrations. The values to the right of each whisker indicate the percentage of test results for that rock unit that exceeds the current EPA action level of 148 Bq/m^3. The WHO and EPA action levels (100 and 148 Bq/m^3, respectively) are also indicated by gray vertical lines for comparison. Summary statistics for all 106 map units are included in the supporting information for this paper (Table S1).

Unlithified clastic surficial deposits (Quaternary alluvium, lacustrine sediments, loess, and glacial drift) and sandstone and siltstone are characterized by generally lower indoor-radon concentrations than carbonate sedimentary (limestone and dolostone) rocks. A Mann-Whitney test showed that the combined clastic surficial, sandstone, and siltstone groups have a significantly lower median than the combined limestone and dolostone groups ($p < 0.001$). Additional Mann-Whitney tests between each pair of lithologic groups showed statistically significant differences in median values ($p < 0.001$) for all pairs except the surficial deposits and sandstone/siltstone ($p = 0.06$). Radon concentrations in homes built on shale spanned the ranges of both the sandstone-siltstone and carbonate units. Although there are differences in radon values by rock unit, there is also considerable overlap. Some high radon values can be found in units with relatively low overall radon values, and some low radon values can be found in units with relatively high overall radon values.

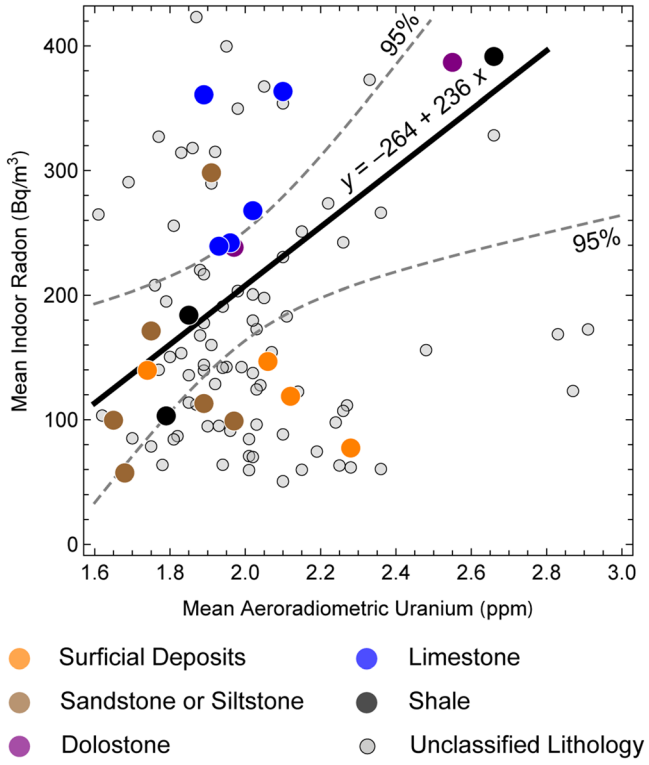

Figure 8. Mean indoor-radon test kit radon concentrations versus mean aeroradiometric uranium concentrations for statewide indoor-radon potential map units. Colored circles represent the 20 monolithologic units shown in Figure 7. Gray circles represent the remaining maps units, which were not classified according to lithology. Regression line and 95% mean confidence bands are for the 20 monolithologic units.

Figure 7 illustrates that, with the exception of one sandstone unit (the Big Clifty Sandstone), there is a well-developed proportional relationship between the means and standard deviations of the log-transformed indoor-radon concentrations for the 20 selected monolithologic units. The best fit line shown on the figure, which omits the labeled outlier, is statistically significant ($p < 0.001$, $r^2 = 0.70$). Moreover, all of the limestone and dolostone units produce indoor-radon concentration means >2.1 log-transformed units (128 Bq/m^3), whereas the sandstone and siltstone units have means <2.0 log-transformed units (93 Bq/m^3). Indoor-radon concentrations in homes built on shale span a wide range of values. In order to better understand the relationship between indoor-radon test kit results and the aeroradiometric uranium values shown in Figure 3, we calculated aeroradiometric uranium zonal statistics (minimum, maximum, mean, median, and standard deviation) for each of the radon geologic map unit polygons and compared them to the indoor test kit results. All other things being equal, we would expect indoor-radon concentrations to be correlated with the aeroradiometric uranium results. The strongest correlation between the test kit radon results and the aeroradiometric uranium data for the 20 selected monolithologic units is between the mean radon and uranium values for each unit ($p = 0.01$, $r^2 = 0.32$). Correlations between median and maximum radon and uranium values for each of the 20 units are weaker ($p = 0.06$, $r^2 = 0.18$ for the median-median comparison; $p = 0.27$, $r^2 = 0.07$ for the maximum-maximum comparison). When all 106 statewide map units are considered, however, the strongest correlation is between the maximum radon and maximum uranium results ($p = 0.10$, $r^2 = 0.03$). Figure 8 illustrates the weakly explanatory but statistically significant relationship between indoor test kit and aeroradiometric mean values for the 20 selected monolithologic units, with points representing the remainder of the map units in the background. Supporting information Table S1 includes summary statistics for both the home test kit radon and aeroradiometric survey uranium values for each of the statewide map units.

Although comparison of the indoor radon and aeroradiometric uranium results shows low overall correlations, there are some results that do compare well. The belt of highest aeroradiometric uranium concentrations in the center of the state corresponds to the Devonian black shale, which has relatively high uranium values (mean: 2.66 ppm, median 2.68 ppm) and also relatively high radon values (mean: 391 Bq/m^3, median 189 Bq/m^3). The Ste. Genevieve Limestone, which shows localized areas of high uranium concentration (Figure 3), also has high unit-wide uranium (mean: 2.19 ppm, median: 2.18 ppm) and radon values (mean: 516 Bq/m^3, median 248 Bq/m^3). Likewise, the Upper Lexington Limestone has both moderately high unit-wide uranium (mean: 1.96 ppm, median: 1.98 ppm) and radon values (mean: 242 Bq/m^3, median 130 Bq/m^3).

4.2. The Statewide Indoor-Radon Potential Map

Our objective in developing a statewide radon potential map was to communicate to homeowners the potential for high radon levels in untested homes in a way that encourages the homeowners to think about testing and, if radon levels are high, mitigate the problem. In plain language, we sought to tell homeowners that, based on what we know from other homes built on the same kind of bedrock, the levels in their untested homes could be as high as the map value. That is a different objective than telling homeowners what the expected value might be or developing statistics for an area-wide risk assessment. Based upon the skewed distributions of indoor-radon values for the units, we chose to characterize the potential for high indoor-radon levels in untested homes using the 75th percentile of each geologic unit. Our choice balances the ideas that, in a positively skewed distribution (like a lognormal distribution), the median, and to some degree the mean, may underrepresent the true potential hazard; conversely, a higher percentile (e.g., the

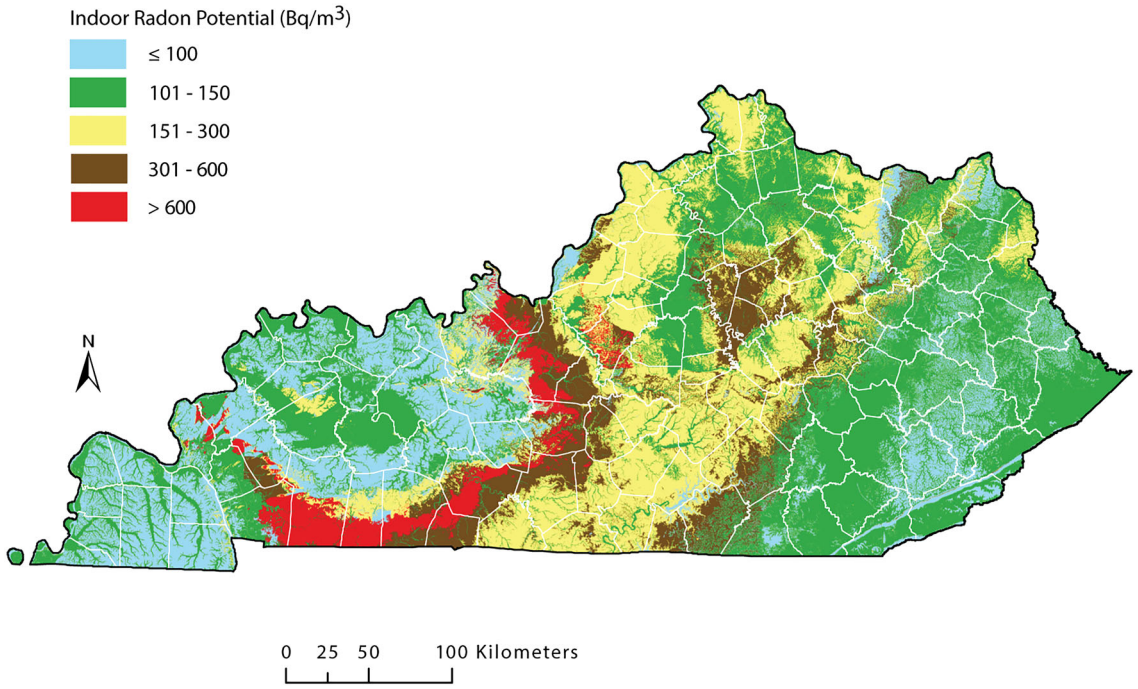

Figure 9. Geologically based indoor-radon potential map of Kentucky. Map category breaks were converted from local customary units of pCi/L (1 pCi/L = 37 Bq/m^3) and rounded upward to the nearest 10 Bq/m^3 to simplify the map legend.

95th or 99th percentile) likely overestimates the potential hazard in most cases. Our choice is also consistent with studies that have found the 75th percentile to be a useful statistic to represent risk in analyses of relationships between radon and lung cancer (Jones, 1995), radon and childhood lymphoma (Peckham et al., 2015), air pollution and placental abruption (Kioumourtzoglou et al., 2019), gestational diabetes and abdominal circumference (Kjos & Schaefer-Graf, 2007), and mercury exposure in rural mining towns (Ohlander et al., 2013).

We grouped the 75th percentile values from the 106 map units into five classes: 0 to 100, 101 to 148, 149 to 296, 297 to 592, and >592 Bq/m^3 to simplify the map (the first two thresholds correspond to WHO and EPA action levels). The result is shown in Figure 9, which conveys information about indoor-radon potential in much more detail than the county-based map shown in Figure 1.

To further make the statewide indoor-radon potential map easy to access and use, we offer it online as an interactive map service maintained by the Kentucky Geological Survey (https://kgs.uky.edu/kygeode/geomap/). The interactive map is tiled for computational efficiency and served using ArcGIS Online in the background, but users need not have access to ArcGIS or any other GIS software. Users can pan, manually zoom to areas of interest, or type a specific street address or geographic location into a search box via their web browser. The interactive map uses pop-up windows that contain hyperlinks to additional information for users who click on specific locations, including a PDF version of a county infographic for the chosen location, the rock unit name and geologic map symbol, and indoor-radon test statistics for that unit (sample size, minimum, maximum, mean, median, and 75th percentile values). The interactive map went online in September 2018 and, as of early September 2020, had 8,784 views for an average of ~12 views per day.

5. Conclusions

Combining observed indoor-radon values and Kentucky's 1:24,000-scale statewide bedrock geology coverage to create a geologically based indoor-radon potential map provides more useful public health information than does the traditional radon map based only on observed radon values with no geological support. Kentucky is the only U.S. state that has its bedrock geology completely mapped at a detailed scale of 1:24,000. However, other entities can integrate whatever geologic maps, regardless of scale, that are available with observed radon values and potentially improve understanding of radon risk potential. In Kentucky,

areas underlain by Ordovician and Mississippian limestones, along with Devonian black shales, have the highest indoor-radon potential. Areas underlain by coarse clastic rocks and surficial deposits tend to have lower indoor-radon potential. Indoor test kit mean values from 20 selected monolithologic units also show a statistically significant correlation with aeroradiometric radon mean values on a formation-by-formation basis. Although the correlation is statistically significant, the aeroradiometric uranium mean values account for only about 32% of the variability of the indoor test kit radon mean values. We attribute the remainder of the variability to a combination of geologic details (e.g., proximity to faults or sinkholes), home construction and foundation integrity, test kit locations within homes, and the inevitable variability introduced by short-term testing. This is an ongoing topic of research within our group. In other geologic settings, high indoor-radon potential may be associated with granitic igneous rocks, alluvium, or glacial deposits. Therefore, although our general approach of combining geology and radon test results can be used in other areas, the results may be different.

Geologically based indoor-radon potential maps such as the one described in this paper are visual representations of radon risk potential based upon the natural factors that control radon emission. This is a substantial improvement over maps depicting only observed radon values or countywide averages. Integrating user-friendly, geologically based interactive radon-potential maps with effective messaging has the potential to reduce exposure to radon and tobacco smoke and, ultimately, the human and economic costs of lung cancer.

Development of our statewide indoor-radon potential map has yielded a number of hypotheses regarding important geological controls on indoor-radon levels that may prove to be fruitful topics for future research. Several are listed below.

The range of radon values for homes built on the five limestones examined suggests that karst development is more important than phosphate mineral content in controlling radon distribution in those units. For example, the Ordovician Lexington Limestone has known phosphate deposits (Cressman, 1973) but has radon values generally lower than the Mississippian Ste. Genevieve and St. Louis Limestones. The Ste. Genevieve Limestone has more caves and sinkholes than the St. Louis Limestone, however, and karst conditions are generally much better developed in these units than in the Lexington Limestone or Louisville Limestone (Paylor & Currens, 2002). Mississippian limestones also have, in general, aeroradiometric uranium values less than, but indoor-radon values higher than, those of Devonian shales (Duval et al., 1993). Karst conduits and sinkholes beneath the surface may allow for rapid migration, trapping, and concentration of available radon gas (Otton, 1992; U.S. Environmental Protection Agency, 1986, 2012). More site-specific work is needed to test the variability in radon concentrations in different types of karst features and landscapes in Kentucky or to see if other mechanisms may result in relatively higher radon potential in limestone.

Dolostones are carbonate rocks but have less susceptibility to karst development than most limestones, so if karst development is influencing radon levels in Kentucky's carbonate rocks, then dolostones should have less radon potential overall than limestones. Our results concerning differences between dolostones and limestones are equivocal. Limestone thickness and chemistry influence karst development, and other factors could be compared between dolostone and limestone units in similar areas to better understand radon potential in Kentucky's carbonate bedrock.

Devonian shales have the highest aeroradiometric uranium values but only the third-highest indoor-radon potential in Kentucky. Other shales have relatively low potential. High radon values for the Devonian shales are likely caused by their high organic content, which is associated with higher trace amounts of uranium and phosphates, than for the other shales examined. Shales, in general, have more clay content and less permeability than limestones (especially karst-influenced limestones), so may have lower radon potential than limestones in the state because migration of radon gases is inhibited by the low permeability of shale. Future comparisons of radon values to organic content, or radon values to fracture locations, may help improve understanding of radon variability in areas of shale bedrock.

The relatively low but variable radon values for sandstone and siltstone units are likely a function of their permeability and organic content. Some sandstones are well cemented and relatively impermeable, whereas others are less well cemented and are reservoirs for water, oil, and gas. Units that have had oil or gas migration or accumulation, such as the Upper Mississippian Big Clifty Sandstone, may have an increased likelihood for uranium and radon decay relative to more well-cemented, nonreservoir sandstones (the Big Clifty Sandstone had the largest variability of the 20 units we examined in detail). Sand grain sizes and

natural cements in the different sandstones mapped also vary, which would influence near-surface permeability. More work is needed to understand radon mobility in near-surface sandstones in Kentucky.

Conflict of Interest

The authors declare no conflicts of interest relevant to this study.

Data Availability Statement

The digital geology coverage used in this paper is publicly available through the Kentucky Geological Survey website (http://kgs.uky.edu). The radon test result data set is not publicly available because of a confidentiality agreement with the radon testing labs but is available from the BREATHE program within the University of Kentucky College of Nursing (http://www.uky.edu/breathe) upon reasonable request.

Acknowledgments

This project was supported in part by UK-CARES through Grant P30 ES026529, the Kentucky Department for Public Health Radon Program, and the Kentucky Geological Survey (a state-supported research center at the University of Kentucky). The contents of this paper are solely the responsibility of the authors and do not necessarily represent the official views of any of the funding agencies. We are grateful to Bethany Overfield for her work to develop the collaboration that led to the statewide radon-potential map, Emily Morris for GIS and graphics support, and Meg Smath for copy editing the manuscript. We also appreciate the comments of two anonymous reviewers and Associate Editor Vengosh, whose input helped to clarify several aspects of the paper. Commercial product names used in this paper are for informational purposes only and do not constitute an endorsement by the authors or their organizations.

References

Al-Zoughool, M., & Krewski, D. (2009). Health effects of radon: A review of the literature. *International Journal of Radiation Biology*, *85*, 57–69. https://doi.org/10.1080/09553000802635054

American Cancer Society (2019). *Cancer facts and figures 2019*. Atlanta, GA: American Cancer Society. Retrieved from https://www.cancer.org/content/dam/cancer-org/research/cancer-facts-and-statistics/annual-cancer-facts-and-figures/2019/cancer-facts-and-figures-2019.pdf

Anderson, W. H., Sparks, T. N., & Weisenfluh, G. A. (2004). Completion of the first phase of the Kentucky digital geologic mapping program. In *Digital mapping techniques '04—Workshop proceedings* (U.S. Geological Survey Open-File Report 2004–1451). Washington, DC: U.S. Geological Survey. Retrieved from https://pubs.usgs.gov/of/2004/1451/anderson/index.html

Barros, N., Steck, D. J., & Field, R. W. (2016). Utility of short-term basement screening radon measurements to predict year-long residential radon concentrations on upper floors. *Radiation Protection Dosimetry*, *171*, 405–413. https://doi.org/10.1093/rpd/ncv416

Barros, N. G., Steck, D. J., & Field, R. W. (2014). A comparison of winter short-term and annual average radon measurements in basements of a radon-prone region and evaluation of further radon testing indicators. *Health Physics*, *106*, 535–544. https://doi.org/10.1097/HP.0000000000000004

Burns, S. F., Ashbaugh, S. G., Paris, R., & Toombs, G. (1998). Presentation of radon potential maps to the public: A case history for Portland, Oregon. *Reviews in Engineering Geology*, *12*, 43–52. https://doi.org/10.1130/REG12-p43

Chiavacci, S. J., Shapiro, C. D., Pindilli, E. J., Casey, C. F., Rayens, M. K., Wiggins, A. T., et al. (2020). Economic valuation of health benefits from using geologic data to communicate radon risk potential. *Environmental Health*, *19*, 1–9. https://doi.org/10.1186/s12940-020-00589-8

Coveney, R. M. Jr., & Glascock, M. D. (1989). A review of the origins of metal-rich Pennsylvanian black shales, central U.S.A., with an inferred role for basinal brines. *Applied Geochemistry*, *4*(4), 347–367. https://doi.org/10.1016/0883-2927(89)90012-7

Cressman, E. R. (1973). Lithostratigraphy and depositional environments of the Lexington Limestone (Ordovician) of central Kentucky. (Professional Paper 768). Washington, DC: U.S. Geological Survey.

Cressman, E. R., & Noger, M. C. (1981). *Geologic mapping of Kentucky; a history and evaluation of the Kentucky Geological Survey-U.S. Geological Survey Mapping Program, 1960–1978 (Circular 801)*. Washington, DC: U.S. Geological Survey.

Currens, J. C. (2002). *Kentucky is karst country! What you should know about sinkholes and springs. (Information Circular 4, Series 12).* Lexington, KY: Kentucky Geological Survey.

Dai, D., Neal, F. B., Diem, J., Deocampo, D. M., Stauber, C., & Dignam, T. (2019). Confluent impact of housing and geology on indoor radon concentrations in Atlanta, Georgia, United States. *Science of the Total Environment*, *668*, 500–5511. https://doi.org/10.1016/j.scitotenv.2019.02.257

Dicken, S. N. (1935). Kentucky karst landscapes. *Journal of Geology*, *43*, 708–728.

Duval, J. S., Carson, J. M., Holman, P. B., & Darnley, A. G. (1993). *Terrestrial radioactivity and gamma-ray exposure in the United States and Canada (Open-File Report 2005–1413)*. Washington, DC: U.S. Geological Survey.

Eble, C. F., & Hower, J. C. (1997). Coal quality trends and distribution of potentially hazardous trace elements in eastern Kentucky coals. *Fuel*, *76*(8), 711–715. https://doi.org/10.1016/S0016-2361(96)00191-3

Florică, Ş., Burghele, B., Bican-Brişan, N., Begy, R., Codrea, V., Cucoş, A., et al. (2020). The path from geology to indoor radon. *Environmental Geochemistry and Health*, *42*(9), 2655–2665. https://doi.org/10.1007/s10653-019-00496-z

Franczyk, J. J., Niewendorp, C. A., & McClaughry, J. D. (2018). Radon potential in Oregon. (open-file report O-18-01). Portland, OR: Oregon Department of Geology and Mineral Industries. Retrieved from https://www.oregongeology.org/pubs/ofr/p-O-18-01.htm

Groves-Kirkby, C. J., Denman, A. R., Crockett, R. G., Phillips, P. S., Woolridge, A. C., & Gillmore, G. K. (2006). Time-integrating radon gas measurements in domestic premises: Comparison of short-, medium- and long-term exposures. *Journal of Environmental Radioactivity*, *86*(1), 92–109. https://doi.org/10.1016/j.jenvrad.2005.07.008

Hahn, E. J., Gokun, Y., Andrews, W. M. Jr., Overfield, B. L., Robertson, H., Wiggins, A., & Rayens, M. K. (2015). Radon potential, geologic formations, and lung cancer risk. *Preventive Medicine Reports*, *2*, 342–346. https://doi.org/10.1016/j.pmedr.2015.04.009

Harvey, R. D. (1984). *Mineral matter and trace elements in the Herrin and Springfield Coals, Illinois Basin Coal Field. (Contract/Grant Report 1983-04)*. Champaign, IL: Illinois State Geological Survey.

Jones, R. L. (1995). Soil uranium, basement radon and lung cancer in Illinois, USA. *Environmental Geochemistry and Health*, *17*(1), 21–24. https://doi.org/10.1007/BF00188627

Karathanasis, A. D. (1991). Phosphate mineralogy and equilibria in two Kentucky Alfisols derived from Ordovician limestones. *Soil Science Society of America Journal*, *55*(6), 1774–1782. https://doi.org/10.2136/sssaj1991.03615995005500060045x

Kentucky Cancer Registry. (2017). Age-adjusted invasive cancer incidence rates by county in Kentucky, 2011–2015. Retrieved from https://www.cancer-rates.info/ky

Kepferle, R. C. (1971). *Members of the Borden Formation (Mississippian) in north-central Kentucky (Bulletin 1354-B)*. Washington, DC: U.S. Geological Survey.

Kioumourtzoglou, M., Huang, Y., Mittleman, M., Ross, Z., Williams, M., Friedman, A., et al. (2019). Air pollution and risk of chronic placental abruption: A study of births in New York City, 2008–2014. *Environmental Epidemiology*, *3*, 206–207. https://doi.org/10.1097/01.EE9.0000608108.52731.e1

Kjos, S. L., & Schaefer-Graf, U. M. (2007). Modified therapy for gestational diabetes using high-risk and low-risk fetal abdominal circumference growth to select strict versus relaxed maternal glycemic targets. *Diabetes Care*, *30*(Supplement 2), S200–S205. https://doi.org/10.2337/dc07-s216

Lagarde, F., Axelsson, G., Damber, L., Mellander, H., Nyberg, F., & Pershagen, G. (2001). Residential radon and lung cancer among never-smokers in Sweden. *Epidemiology*, *12*(4), 396–404. https://doi.org/10.1097/00001648-200107000-00009

Leventhal, J. S. (1981). Pyrolysis gas chromatography-mass spectrometry to characterize organic matter and its relationship to uranium content of Appalachian Devonian black shales. *Geochimica et Cosmochimica Acta*, *45*(6), 883–889. https://doi.org/10.1016/0016-7037(81)90116-2

Leventhal, J. S., & Hosterman, J. W. (1982). Chemical and mineralogical analysis of Devonian black-shale samples from Martin County, Kentucky; Carroll and Washington Counties, Ohio; Wise County, Virginia; and Overton County, Tennessee, USA. *Chemical Geology*, *37*(3–4), 239–264. https://doi.org/10.1016/0009-2541(82)90081-X

McDowell, R. C. (1986). *The geology of Kentucky; A text to accompany the geologic map of Kentucky (Professional Paper 1151-H)*. Washington, DC: U.S. Geological Survey.

McFarlan, A. C. (1943). *Geology of Kentucky*. Lexington, KY: University of Kentucky.

Mendez, D., Alshanqueety, O., Warner, K. E., Lantz, P. M., & Courant, P. N. (2011). The impact of declining smoking on radon-related lung cancer in the United States. *American Journal of Public Health*, *101*(2), 310–314. https://doi.org/10.2105/AJPH.2009.189225

Miles, J. C. H., & Appleton, J. D. (2005). Mapping variation in radon potential both between and within geological units. *Journal of Radiological Protection*, *25*(3), 257–276. https://doi.org/10.1088/0952-4746/25/3/003

Ohlander, J., Huber, S. M., Schomaker, M., Heumann, C., Schierl, R., Michalke, B., et al. (2013). Risk factors for mercury exposure of children in a rural mining town in northern Chile. *PLOS ONE*, *8*, e79756. https://doi.org/10.1371/journal.pone.0079756

Otton, J. K. (1992). *The Geology of Radon*. Washington, DC: U.S. Geological Survey.

Overfield, B. L., Andrews, W. M., Robertson, H., Rayens, M. K., & Hahn, E. J. (2016). Radon research collaboration between the Kentucky Geological Survey and the University of Kentucky College of Nursing: An innovative partnership. In *Special Papers* (Vol. 520, pp. 267–271). Boulder, CO: Geological Society of America. https://doi.org/10.1130/2016.2520(23)

Palmer, A. N. (1989). Stratigraphic and structural control of cave development and groundwater flow in the Mammoth Cave region. In *Karst hydrology: Concepts from the Mammoth Cave area* (pp. 293–316). New York: Van Nostrand Reinhold Publishers.

Paylor, R. L., & Currens, J. C. (2002). *Karst occurrence in Kentucky (Map and Chart 33, series 12)*. Lexington, KY: Kentucky Geological Survey.

Peckham, E. C., Scheurer, M. E., Danysh, H. E., Lubega, J., Langlois, P. H., & Lupo, P. J. (2015). Residential radon exposure and incidence of childhood lymphoma in Texas, 1995–2011. *International Journal of Environmental Research and Public Health*, *12*, 12,110–12,126. https://doi.org/10.3390/ijerph121012110

Perkins, R. B., & Mason, C. E. (2015). The relative mobility of trace elements from short-term weathering of a black shale. *Applied Geochemistry*, *56*, 67–79. https://doi.org/10.1016/j.apgeochem.2015.01.014

Phillips, J. D., Duval, J. S. & Ambroziak, R. A. (1993). National geophysical data grids; gamma-ray, gravity, magnetic, and topographic data for the conterminous United States (Data Series. 9). US Geological Survey https://doi.org/10.3133/ds9

Schumann, R. R. (Ed) (1993). *Geologic radon potential of EPA Region 4 (Open-File Report 93-292-D)*. Washington, DC: U.S. Geological Survey.

Smethurst, M. A., Strand, T., Sundal, A. V., & Rudjord, A. L. (2008). Large-scale radon hazard evaluation in the Oslofjord region of Norway utilizing indoor radon concentrations, airborne gamma ray spectrometry and geological mapping. *Science of the Total Environment*, *407*(1), 379–393. https://doi.org/10.1016/j.scitotenv.2008.09.024

Stanley, F. K. T., Irvine, J. L., Jacques, W. R., Salgia, S. R., Innes, D. G., Winquist, B. D., et al. (2019). Radon exposure is rising steadily within the modern North American residential environment, and is increasingly uniform across seasons. *Nature Scientific Reports*, *9*(1), 1–17. https://doi.org/10.1038/s41598-019-54891-8

Sundal, A., Henriksen, H., Soldlal, O., & Strand, T. (2004). The influence of geological factors on indoor radon concentrations in Norway. *Science of the Total Environment*, *328*(1–3), 41–53. https://doi.org/10.1016/j.scitotenv.2004.02.011

Swanson, R. W. (1961). *Geology and geochemistry of uranium in marine black shales: A review (Professional Paper 356-C)*. Washington, DC: U.S. Geological Survey.

Tanner, A. B. (1986). *Indoor radon and its sources (Open-file report 86-222)*. Washington, DC: U.S. Geological Survey.

Udgata, D. B. P. (2011). Depositional and stratigraphic significance of marine, green-clay, mineral facies in the lower-middle Mississippian Borden and Fort Payne Formations, western Appalachian and eastern Illinois basins, Kentucky (Doctoral dissertation). Retrieved from UKnowledge. (https://uknowledge.uky.edu/gradschool_diss/808). Lexington, KY: University of Kentucky.

U.S. Department of Health and Human Services, Centers for Disease Control and Prevention (2018). Extinguishing the tobacco epidemic in Kentucky. Retrieved from https://www.cdc.gov/tobacco/about/osh/program-funding/pdfs/kentucky-2018-508.pdf

U.S. Environmental Protection Agency (1986). *A citizen's guide to radon: What it is and what to do about it. (OPA-86-004)*. Washington, DC: U.S. Environmental Protection Agency.

U.S. Environmental Protection Agency. (1993). EPA map of radon zones—National summary. In Air and radiation (6604J), 402-R-93-071.

U.S. Environmental Protection Agency (2009). *A citizen's guide to radon: The guide to protecting yourself and your family from radon. (Report 402-K-09-001)*. Washington, DC: Environmental Protection Agency.

U.S. Environmental Protection Agency (2012). *A citizen's guide to radon: The guide to protecting yourself and your family from radon. (EPA402/K-12/002)*. Washington, DC: U.S. Environmental Protection Agency.

Vienneau, D., de Hoogh, K., Hauri, D., Vicedo-Cabrera, A. M., Schindler, C., Huss, A., et al. (2017). Effects of radon and UV exposure on skin cancer mortality in Switzerland. *Environmental Health Perspectives*, *125*, 067009. https://doi.org/10.1289/EHP825

VoPham, T., DuPré, N., Tamimi, R. M., James, P., Bertrand, K. A., Vieira, V., et al. (2017). Environmental radon exposure and breast cancer risk in the nurses' health study II. *Environmental Health*, *16*, 97. https://doi.org/10.1186/s12940-017-0305-6

Weir, G. W., Gualtieri, J. L., & Schlanger, S. O. (1966). *Borden formation (Mississippian) in south- and south-central Kentucky. (Bulletin 1224-F)*. Washington, DC: U.S. Geological Survey.

White, W. B., Watson, R. A., Pohl, E. R., & Brucker, R. (1970). The central Kentucky karst. *Geographical Review*, *60*, 88–115.

Zhukovsky, M., Yarmoshenko, I., & Kiselev, S. (2012). Combination of geological data and radon survey results for radon mapping. *Journal of Environmental Radioactivity*, *112*, 1–3. https://doi.org/10.1016/j.jenvrad.2012.02.013